

MEASUREMENTS OF HIGH-PRESSURE STEAM-WATER ENTHALPY/VOID MIGRATION IN UNEQUALLY HEATED HORIZONTAL TWIN SUBCHANNELS

Document No. CW-125130-CONF-001

S.C. Sutradhar

S.T. Yin¹

R.M. Tain²

Atomic Energy of Canada Limited
Chalk River Laboratories, Chalk River, Ontario Canada K0J 1J0
E-mail: sutradhars@aecl.ca

¹ Presently, Consultant for Atomic Energy of Canada Limited-SP
28 Ridgecrest Drive, Toronto, Ontario Canada M1W 4A2
E-mail: yinst@sympatico.ca

² Presently at Industrial Technology Research Institute
Chutung, Hsinchu, Taiwan 310 ROC
E-mail: rtain@itri.org.tw

ABSTRACT

An experimental study of enthalpy/void migration in two interconnected, unequally heated horizontal subchannels was conducted using high-pressure steam-water as the operating medium. The cross-sectional geometry of the twin subchannels simulated two adjacent, top-to-bottom aligned inner subchannels of a 37-element CANDU^{®3} fuel bundle. The effect of unequal heating on enthalpy/void migration was measured using three different heat flux ratios of 1.00, 1.11 and 1.21, with the higher heat flux in the top subchannel. The test results indicated that under similar flow conditions, the unequal heat flux set-up enhanced the enthalpy/void migration from the bottom to the top subchannel compared to the equal heat flux set up. This study quantifies and characterizes the buoyancy-induced enthalpy/void migration between two interconnected horizontal subchannels subject to different heat fluxes. The database will be used to validate and improve the flow-mixing models in subchannel codes.

1. INTRODUCTION

The prediction of flow, steam quality and void distribution in the subchannels of a horizontally oriented CANDU fuel bundle is of importance in design and safety analyses of CANDU reactors. The cross-sectional variation of these physical quantities in the fuel bundles need to be accurately predicted under normal and off-normal conditions, as the fuel bundle's heat transfer behaviour, dryout power/location and the operating limits are directly affected by these physical parameters.

The present work is a continuation of the two previous studies by Yin et al. (1990, 1999) in which measurements were conducted with equal heat flux applied to the interconnected twin subchannels. The objective of this study is to quantify and characterize the buoyancy-induced enthalpy/void migration between two interconnected horizontal subchannels subject to different heat fluxes. Measurements were

³ CANDU[®]: (CANada Deuterium Uranium) is a registered trademark of Atomic Energy of Canada Limited (AECL)

made using a high-pressure steam-water mixture at typical CANDU reactor operating conditions. The cross-sectional geometry of the test section simulated two adjacent, top-to-bottom-aligned inner subchannels of a CANDU 37-element fuel bundle. The database will be used to validate some of the subchannel codes, and to improve the subchannel mixing models in these codes.

2. LITERATURE REVIEW

In the past, a large number of experimental studies were conducted to investigate the flow-mixing phenomenon and the enthalpy/void distribution in the nuclear reactor fuel subchannels. Air-water mixture and flow-boiling water were used as the working fluids in both vertical and horizontal flow orientations. Rudzinski et al. (1972), Shoukri et al. (1984), Tapucu et al. (1990), Osamusali et al. (1992) and Sadatomi et al. (1997) reported tests with air-water flow. Tests with boiling-water present a much greater challenge to the researchers due to the technical complexities at high-pressure and high-temperature test conditions. Rowe and Angle (1967, 1969) were among the first to measure flow and enthalpy distribution in single-phase and boiling water (6.2 MPa) using two interconnected vertical channels simulating two adjacent subchannels of a 19-rod bundle. The results indicated that mixing during boiling was found to be dependent upon the rod spacing, flow rate and, possibly, steam quality. Lahey Jr. et al. (1972) measured flow and enthalpy distribution in a 9-rod cluster at the boiling water reactor (BWR) pressure (6.9 MPa). Barber and Zielke (1980), Herkenrath et al. (1981), Fighetti and Reddy (1982), and Wang and Cao (1993) obtained flow and enthalpy-mixing data at pressurized water reactor (PWR) coolant-flow conditions, using square-array subchannels of 24-, 16- and 9-rod bundles.

All the afore-mentioned water tests dealt with vertical up-flow without considering the buoyancy effect on the mixing phenomenon. A recent literature survey by Yu et al. (1998) on the modelling of two-phase flow in interconnected subchannels indicated that Yin et al. (1990, 1999) and Carver et al. (1995) appeared to be the only researchers in recent years engaged in the experiments and analysis of high-pressure steam-water mixing and enthalpy distribution in horizontal flow systems.

3. EXPERIMENTAL SET-UP

3.1 Test Facility and Instrumentation

The MR-1A high-pressure water loop at the Chalk River Laboratories was used for the present experiment. The test section was heated by a DC power supply of 350-kW capacity (175 V x 2000 A). Figure 1 shows a schematic of the twin subchannels flow circuits. The test section flow area simulated two adjacent, top-to-bottom aligned inner subchannels of a 37-rod fuel bundle, as shown in Figure 2. The directly heated test section consisted of two identical Inconel 625 tubular heaters of 6.35-mm O.D. and 0.89-mm wall thickness with a total heated length of 3.0 m.

Each heater tube was milled with a 1.78-mm-wide by 3.0-m long slot over the entire heated length. At both the upstream and downstream ends of the 3.0 m heated length, there were un-machined portions of the same Inconel 625 tube for entrance and exit connections. The slots of both heaters were facing each other with a 1.99-mm uniform gap between them to facilitate mixing of the boiling two-phase mixtures between the heaters. Figure 3 shows the cross-sectional view of the twin, interconnected subchannels. The heaters were encased in two strings of symmetrically grooved semi-cylindrical alumina insulators. The assembly was placed in a heavy-walled 304 stainless-steel tube for the high-pressure operation. At the end of the heated length, the twin subchannel flows were isolated from each other for separate discharge to their respective condensers.

The main features of the test-section design were: i) no intrusive objects in the heated subchannels, ii) full-flow collection from each subchannel for calorimetric evaluation, iii) high degree of symmetry in the subchannels and the condenser circuits, and iv) variation of heat flux ratios in the subchannels.

The instrumentation arrangements for the heated test section and the downstream twin condenser circuits are also shown in Figure 1. Rosemount absolute and differential pressure cells were used to measure the test-section outlet pressure and the pressure drops across the venturi flow meters, respectively. All pressure cells were calibrated against a standard with an accuracy of $\pm 0.025\%$ to $\pm 0.65\%$ of the operating range, depending on the measurement locations. The subchannel fluid bulk temperatures at the inlet and outlet were measured with stainless-steel sheath K-type thermocouples. The condensers' shell-side inlet and outlet temperatures were measured using high-accuracy resistance temperature detectors, calibrated to an accuracy of $\pm 0.1^\circ\text{C}$. A desktop computer equipped with digital and graphic display software was used for controlling the loop conditions. The same system was employed for data acquisition.

The measurement uncertainties were recorded in basic physical quantities (such as coolant temperature, pressure and test section power) as well as in computed quantities (such as mass flux, heat flux and heat balance etc.). These were mainly instrument output fluctuations observed during the tests with reference to the desired operating conditions. The averaged measurement uncertainties within the test range are summarized as follows: flow rates $\pm 0.46\%$; mass flux $\pm 0.83\%$; temperature $\pm 0.55\%$ (RTDs) and $\pm 0.5\%$ (thermocouples); pressure $\pm 0.025\%$ (test section exit) and $\pm 0.65\%$ (test section pressure drop); power to test section $\pm 0.25\%$; heat flux $\pm 0.6\%$; heat balance within the test section $\pm 2.0\%$ (10 to 60 kW applied to the 3.0 m heated length); test section heat loss (at $3.0 \text{ Mg/m}^2\text{s}$ flow and 250°C) $\approx 0.5 \text{ kW}$; enthalpy and enthalpy differential within $\pm 0.25\%$ (based on condenser tube-shell heat balance test).

3.2 Variation of Heat Flux Between Twin Subchannels

To generate unequal heat flux between the twin subchannels, a water-cooled external variable resistor was connected in series to the downstream end of the bottom subchannel heater to restrict the current passing through it. The resistor was made of the same material as the subchannel heaters (Inconel 625 tubing, 6.35-mm O.D. and 0.89-mm wall thickness). Varying the length of the resistor changed the electrical current passing through the bottom subchannel thus controlled the heat flux ratio between the twin subchannels. Three heat-flux ratios ($R = 1.00, 1.11$ and 1.21) were used for the present tests, with the top subchannel being at the higher power. In the present study, most of the tests were conducted with $R = 1.21$ which was considered more pertinent for code analysis. The case of $R = 1.00$ (i.e., equal heating) was included for the "tie-back" runs so that comparisons could be made with previously obtained data (Yin et al. 1999) using the same test assembly under equal heating conditions. The case of $R = 1.11$ was performed with very limited number of runs to check the sensitivities of unequal heating.

3.3 Test Matrix and Procedure

The test matrix was similar to that of the previously conducted equal heat-flux tests, which was designed to include the nominal CANDU reactor operating conditions plus some extended ranges to examine the parametric effects. The test matrix for the unequal heat flux test was as follows:

Heat-flux ratio (R)	= 1.00, 1.11, 1.21 (top/bottom subchannel)
Pressure (P)	= 5.0 and 10.0 MPa (at test-section exit)
Mass flux (G)	= 1.6, 2.0, 2.5, 3.0 $\text{Mg/m}^2\text{s}$ (each subchannel)
Inlet subcooling (ΔT_{in})	= 40°C to 60°C
Power (q)	= 5 to 100 kW (at 2.5 to 10 kW increment)

3.4 Test Procedure

Single-phase heat-balance tests within the 3.0-m long heated subchannels (i.e., electrical heat input compared to water enthalpy gain) and between the tube- and shell-side of each condenser were conducted prior to two-phase measurements. The heat-flux ratio was established during calibrations runs as described in Section 3.2. The test-section outlet pressure, mass flux and inlet temperature were adjusted to the desired conditions. The tests were conducted using equal flows (measured at the outlet of the test section) in the subchannels and data were taken at steady state after each power increment. The power steps varied from 2.5 to 10 kW, depending on low or high flow rates and the trend of the enthalpy/void migration curve. The enthalpy/void migration from the bottom to the top subchannel was calculated by taking the difference of the total energy carried in each subchannel between the outlets (TE03 and TE04) and the downstream mixing joint (TE08); i.e., $(\Delta h_1 + \Delta h_3) - (\Delta h_2 + \Delta h_4)$, as illustrated in Figure 1. Note that Δh_1 and Δh_2 were measured by the enthalpy increase in the shell-side of the twin condensers.

4. RESULTS AND DISCUSSIONS

4.1 Effect of Heat-Flux Ratio

The effect of unequal heating on enthalpy/void migration from the bottom to top subchannel was presented by plotting the specific enthalpy difference (top subtracting bottom) against the average exit quality (X_{ave}) using the heat flux ratios of $R = 1.00$ and $R = 1.21$. Figures 4 to 6 show the results at 5.0 MPa for the three mass fluxes of 2.0, 2.5 and 3.0 Mg/m²s. The effect of the extra heat flux in the top subchannel was clearly observed. A bell-shaped migration curve was observed for each test series, with a peak value located at $X_{ave} \approx 7.5\%$. In the peak regions, the unequal heating tests showed an enthalpy/void migration enhancement by about 150% to 300% compared to the equal heating tests. The enhancement was proportional to the increment of mass flux. In the non-boiling or subcooled boiling region, where $X_{ave} < 0\%$, the enthalpy/void migration was small and the unequal and equal heating results were similar. As the X_{ave} increased beyond the peak region, the enthalpy/void migration curves for both equal and unequal heating decreased continuously and eventually converged to similar values at an average exit quality equal or greater 20%.

Figures 7 to 9 show the results from the 10.0 MPa pressure tests with heat-flux ratios at $R = 1.00$, 1.11 and 1.21 covering three mass fluxes of 1.6, 2.0 and 2.5 Mg/m²s. The higher heat fluxes in the top subchannel again induced greater enthalpy/void migration under all flow conditions. At the lowest mass flux of 1.6 Mg/m²s (Figure 7), two peak regions of the enthalpy/void migration appeared to exist. The first peak, which was relatively small in magnitude and more evident for the unequal heating case, was observed at $X_{ave} \approx 10\%$. The second peak, of much greater magnitude and barely noticeable by the peaking behavior of the data trend, appeared to be close to $X_{ave} \approx 60\%$. The heat flux ratio $R = 1.11$ was performed with limited number of runs to check the sensitivities of unequal heating, as pointed out in Section 3.2. As shown in Figure 8, the $R = 1.11$ data string is clearly below the $R = 1.21$ case. The first peak region ($X_{ave} \approx 10\%$) mentioned above was consistently observed at all three mass fluxes of 1.6, 2.0 and 2.5 Mg/m²s for all three heat flux ratios. The peak values for the unequal heating tests were estimated to be about 150% to 200% greater than those of the equal heating tests. For the unequal heating case, the second peak was not yet observable because the exit quality was not high enough. However, the data trend appeared to follow that of the equal heating case.

4.2 Effect of Mass Flux

The effect of mass flux on enthalpy/void migration at 10.0 MPa pressure was displayed in Figure 10 at four mass fluxes of 1.6, 2.0, 2.5, and 3.0 Mg/m²s all under the heat-flux ratio of $R = 1.21$. In the low-quality region (where $X_{ave} < 10\%$ or before the first peak), the enthalpy/void migration results had similar values and were not appreciably affected by the variation of mass flux. It can be stated that from zero quality to the peak region, enthalpy/void migration showed little or no effect due to mass flux variation. In the high-quality region (where $X_{ave} > 10\%$), the enthalpy/void migration curves first decreased to a minimum (at $X_{ave} \approx 20$ to 25%) and then increased again for all four mass fluxes with the lowest mass flux on the top and the highest mass flux at the bottom.

4.3 Effect of System Pressure

Figure 11 shows the effect of system pressure on enthalpy/void migration using a representative mass flux of 2.5 Mg/m²s under unequal heating. Prior to and including the peak regions, the results between 5.0 and 10.0 MPa were similar except that the lower-pressure results peaked at $X_{ave} \approx 7.5\%$ and the higher-pressure results peaked at $X_{ave} \approx 10\%$ as also discussed in section 4.1. Beyond the peaks and in the high quality region, the enthalpy/void migration curve for the 10.0 MPa tests exhibited a minimum at $X_{ave} \approx 20$ to 25% and then continuously increased. Based on the peaking trend observed at $X_{ave} \approx 60\%$ with the 1.6 Mg/m²s and 10.0 MPa (Figure 7), the high-flow 2.5 Mg/m²s case under discussion may reach a second peak if the X_{ave} is sufficiently high. The 5.0 MPa data string generally exhibited a bell-shaped single peak in the low quality region ($X_{ave} \approx 7.5\%$) with a trend approaching to a minimum level with increased exit quality.

5. SUMMARY AND CONCLUSIONS

An experimental study was performed to quantify and characterize the effect of buoyancy-induced migration on void distribution in two interconnected, unequally heated horizontal subchannels at CANDU reactor operating conditions. The database will be used to validate and improve the mixing models in subchannel codes.

The conclusions are as follows.

- 1) Unequal heating of the twin subchannels showed various degrees of impact on the enthalpy/void migration depending on flow and system pressure conditions. Higher heat fluxes in the top subchannel resulted in higher enthalpy/void migration from the bottom to the top subchannel.
- 2) For a fixed subchannel geometry, the heat-flux ratio, mass flux, system pressure and thermodynamic quality (at the subchannel exit) were the major parameters governing the enthalpy/void migration. The migration increased with either decreasing mass flux or increasing system pressure under both equal and unequal heating cases.
- 3) Peak regions were observed in the plots of enthalpy/void migration versus average exit quality (X_{ave}). The lower-pressure (5.0 MPa) tests exhibited a bell-shaped enthalpy/void migration curves and peaked at $X_{ave} \approx 7.5\%$. The higher-pressure (10.0 MPa) tests peaked at $X_{ave} \approx 10\%$ and the migration continued to increase as the exit quality was increased. These peak regions ($X_{ave} \approx 7\%$ and 10%) were probably due to a maximum exchange of liquid and vapour phases between the subchannels where bubbly flow prevailed along the boiling length under such low X_{ave} conditions.
- 4) In the peak region of the 5.0 MPa tests (Figures 4 to 6), the unequal heating enhanced enthalpy/void migration by 150% to 300% compared to the equal heating. Similarly, in the peak region of the 10.0 MPa

tests (Figures 7 to 9), the unequal heating enhanced enthalpy/void migration by 150% to 200%. The enhancement was proportional to the increment of mass flux.

5) The equal heating tests at $1.6 \text{ Mg/m}^2\text{s}$ mass flux and 10.0 MPa pressure appeared to have a second peak region approaching at $X_{\text{ave}} \approx 60\%$ with much higher enthalpy/void migration than the first peak at $X_{\text{ave}} \approx 10\%$ (Figure 7). The unequal heating tests showed peak regions at low exit qualities ($X_{\text{ave}} \approx 7\%$ and 10%) but the signals of a possible second peak were not yet noticeable as the tests were limited at or under $X_{\text{ave}} \approx 45\%$ to avoid dryout conditions.

ACKNOWLEDGEMENTS

The authors wish to acknowledge the joint funding provided by AECL and COG for this work.

REFERENCES

Barber, A.R. and Zielke, L.A., 1980. Subchannel Thermal-hydraulic Experimental Program (STEP): Vol. 1, Mixing in a PWR Bundle. NP-1493.

Carver, M.B, Kiteley, J.C., Zhou, R., Junop, S.V. and Rowe, D.S., 1995. Validation of the ASSERT Subchannel Code: Prediction of Critical Heat Flux in Standard and Nonstandard CANDU Bundle Geometries. Nuclear Technology, 112, pp. 299-314.

Fighetti, C.F. and Reddy, D.G., 1982. Experimental Determination of Subchannel Mass Flow Rate and Enthalpy in Rod Bundles. 1982 AIAA/ASME Joint Fluid, Plasma, Thermophysics and Heat Transfer Conf., St. Louis, Missouri.

Herkenrath, H., Hufschmidt, W., Jung, U. and Weckermann, F., 1981. Experimental Investigation of Enthalpy and Mass Flow-Distribution in 16-Rod Clusters with BWR-PWR-Geometries and Conditions. EUR-7535.

Lahey, R.T. Jr., Shiralkar, B.S., Radcliffe, D.W. and Polomik, E.E., 1972. Out-of-Pile Subchannel Measurements in a 9-Rod Bundle for Water at 1000 psia. Progress in Heat Transfer, 6, Pergamon Press, London, pp. 345-363.

Osamusali, S.L, Groeneveld, D.C. and Cheng, S.C., 1992. Two-Phase Flow Regimes and Onset of Flow Stratification in Horizontal 37-Rod Bundles. Int. J. of Heat and Technology, 10, No. 1, pp. 44-74.

Rowe, D.S. and Angle, C.W., 1967 (Part 2) and 1969 (Part 3). Crossflow Mixing between Parallel Flow Channels during Boiling. BNWL-371.

Rudzinski, K.F., Singh, K. and St. Pierre, C.C., 1972. Turbulent Mixing for Air-Water Flows in Simulated Rod Bundle Geometries. Canadian J. of Chemical Engineering, 50, pp. 297-299.

Sadatom, M., Kawahara, A. and Sato, A., 1997. Lateral Velocities due to Diversion Cross-Flow and Void Drift in a Hydraulically Non-Equilibrium Two-Phase Subchannel Flow. 1997 ASME Fluid Eng. Division. Summer Meeting, June 22-26, pp. 1-7.

Shoukri, M., Tawfik, H. and Chan, A.M.C., 1984. Two-Phase Redistribution in Horizontal Subchannel Flow - Turbulent Mixing and Gravity Separation. Int. J. Multiphase Flow, 10, No. 3, pp. 357-369.

Tapucu, A., Teysseidou, A., Geckinli, M. and Merilo, M., 1990. Axial Pressure Distribution in Two Laterally Interconnected Subchannels with Blockage. *Int. J. of Multiphase Flow*. 16, No. 3, pp. 461-279.
 Wang, J.M. and Cao, L.P., 1993. Experimental Research for Subcooled Boiling Mixing between Subchannels in a Bundle. *NURETH 6*, Vol 1, pp. 663-670.

Yin, S.T. and Snoek, C.W., 1990. Measurement of Enthalpy Migration in a Horizontal Test Assembly with Two Interconnected Subchannels, Canadian Nuclear Society Conf. Proceedings. Toronto.

Yin, S.T., Tain, R.M. and Sutradhar, S.C., 1999. An Experimental Investigation of Enthalpy/Void Migration in an Interconnected Horizontal Twin-Subchannel Assembly, Paper No. 298, Proceedings of NURETH-9, San Francisco.

Yu, R.S., Lightstone, M.F. and Currie, I. G., 1998. On the Modelling of Two-Phase Flow in Interconnected Subchannels - A Literature Review. University of Toronto Technical Report, Mechanical and Industrial Engineering Dept.

NOMENCLATURE

$\Delta h_1, \Delta h_2$	Enthalpy exchange (tube-to-shell, within twin condensers, Fig. 1)	kJ/kg
$\Delta h_3, \Delta h_4$	Enthalpy contents in the downstream subcooled legs (Fig. 1)	kJ/kg
Dhup	Energy transfer rate in top condenser ($\Delta h_1 + \Delta h_3$) x FT02 (Fig. 1)	kJ/s
Dhlow	Energy transfer rate in bottom condenser ($\Delta h_2 + \Delta h_4$) x FT01 (Fig. 1)	kJ/s
dhup = Dhup/FT02		kJ/kg
dhlow = Dhlow/FT01		kJ/kg
DH, (dhup – dhlow) =	Enthalpy migration = (DHup/FT02 – DHlow/FT01)	kJ/kg
FT01	Bottom-subchannel flow rate	g/s
FT02	Top-subchannel flow rate	g/s
FT03	Flow rate shell-side of bottom condenser	g/s
FT04	Flow rate shell-side of top condenser	g/s
G	Mass flux	Mg/m ² s
L	Heated length	m
P, PT01	Pressure at test-section exit	MPa
q	Power to test section	kW
Q	Heat flux	kW/m ²
R	Heat-flux ratio (top subchannel kW/bottom subchannel kW)	
TE	Thermocouple identification	
ΔT_{in}	Inlet subcooling	°C
$T_{in, TE07}$	Test-section inlet temperature	°C
TE08	Temperature at the location where subchannel flows merged	°C
X_{in}	Inlet quality	%
X_{ave}	Average quality at test-section outlet based on DC power input	%

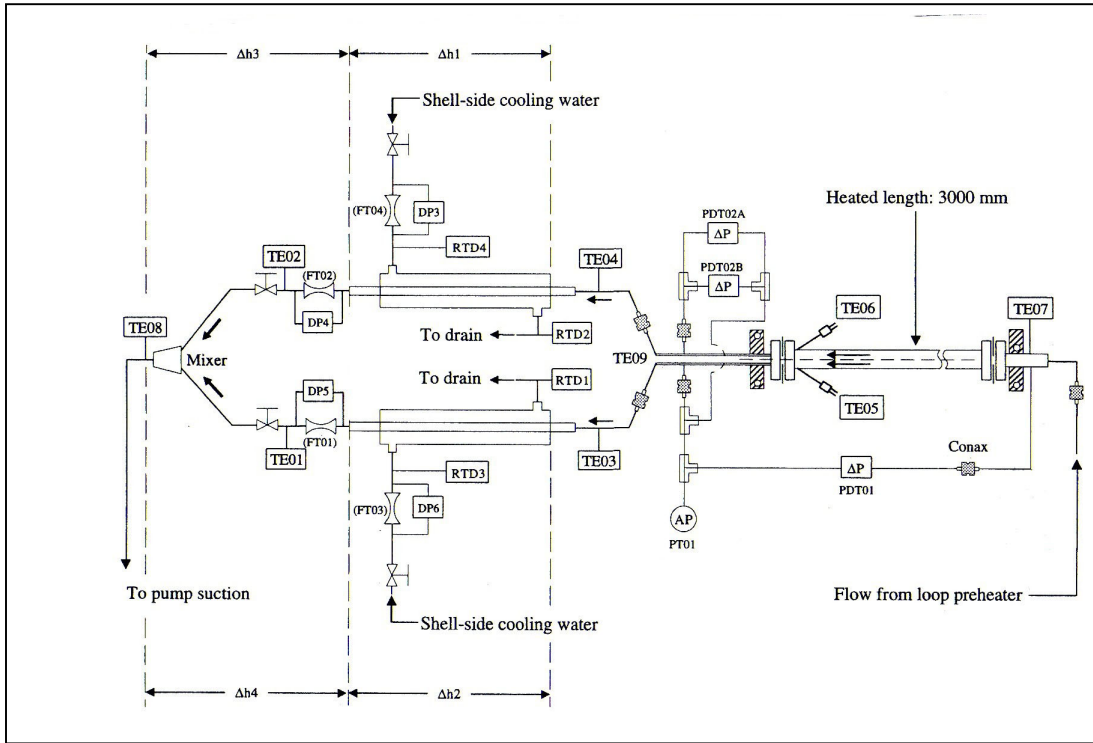


Figure 1: Schematic Diagram of the Twin-Subchannel Flow Circuits

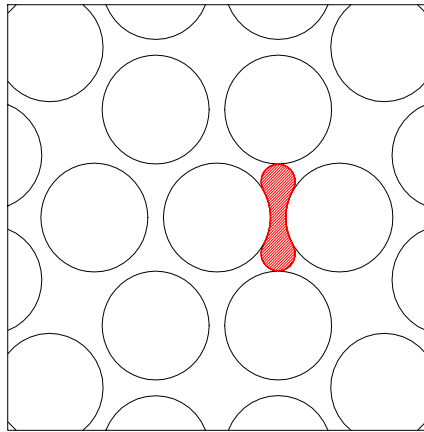


Figure 2: Simulation of the Inner Subchannels of a CANDU 37-Rod Bundle

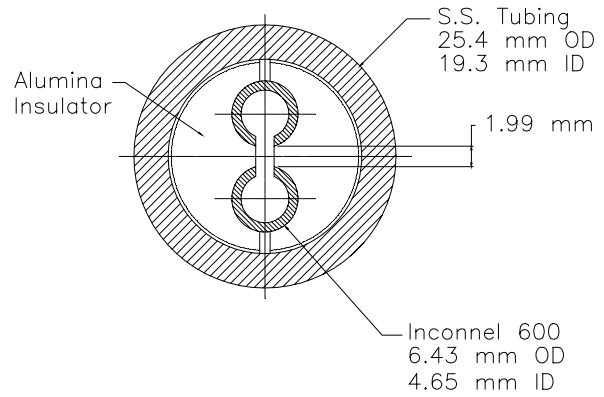


Figure 3: Cross-Sectional View of the Twin Subchannels

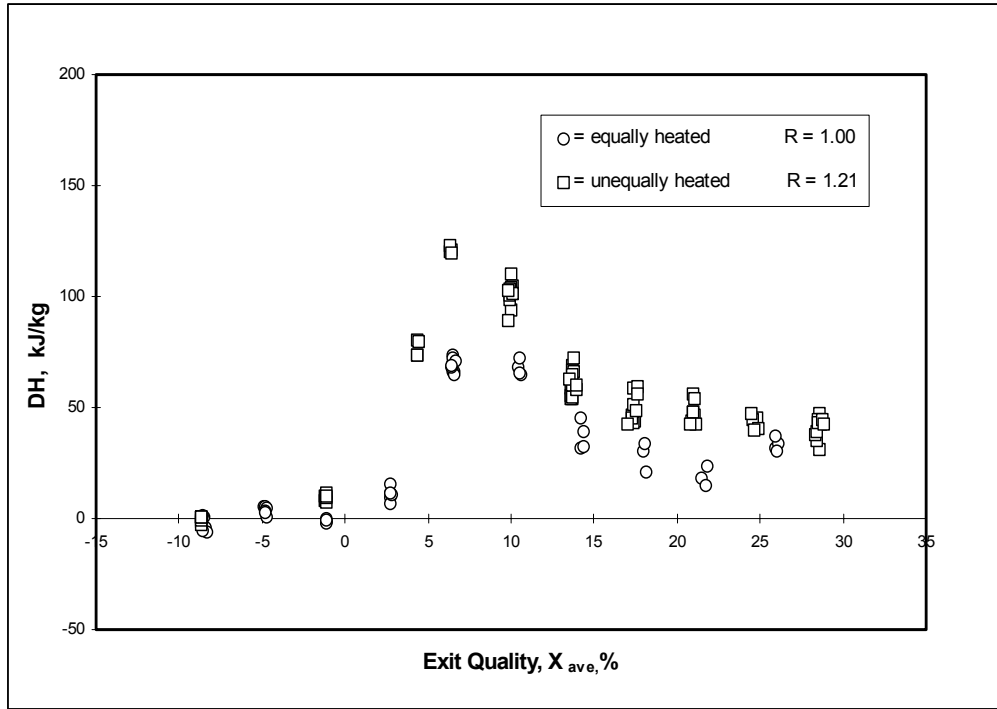


Figure 4: Enthalpy/Void Migration vs. Exit Quality at $P = 5.0$ MPa and $G = 2.0$ Mg/m²s

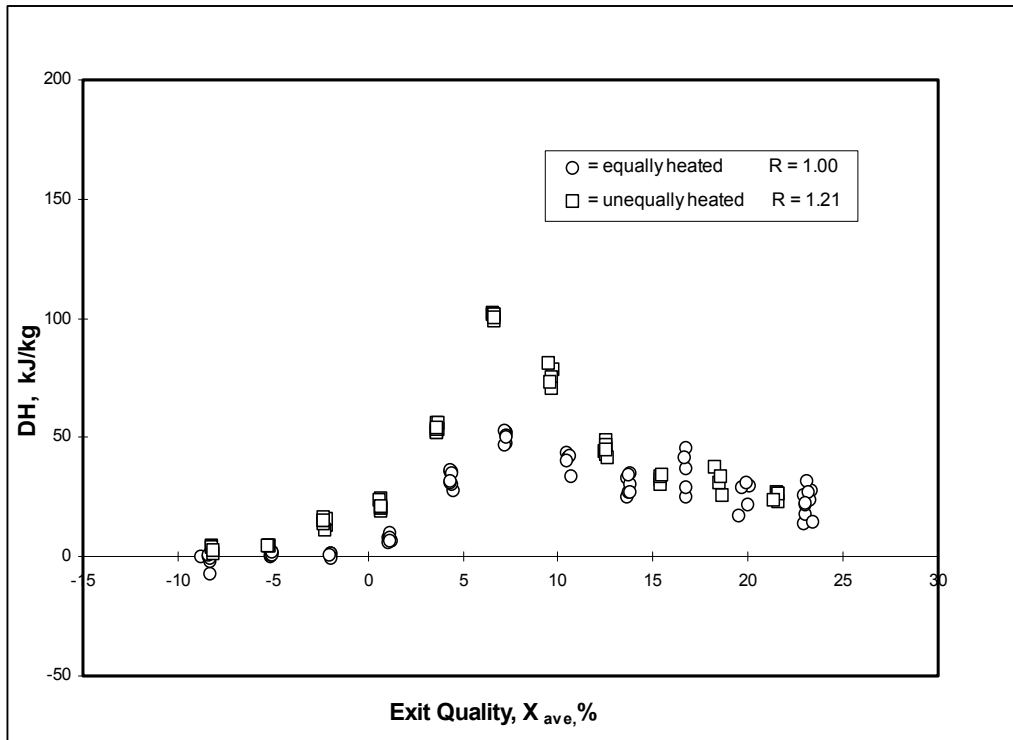


Figure 5: Enthalpy/Void Migration vs. Exit Quality at $P = 5.0$ MPa and $G = 2.5$ Mg/m²s

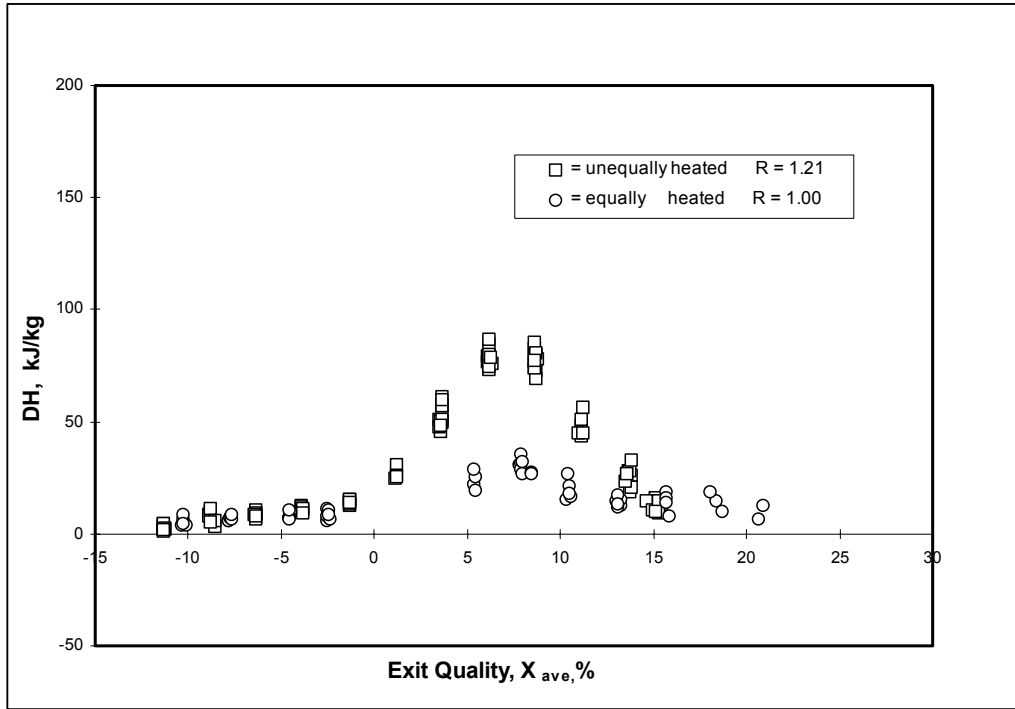


Figure 6: Enthalpy/Void Migration vs. Exit Quality at $P = 5.0$ MPa and $G = 3.0$ Mg/m²s

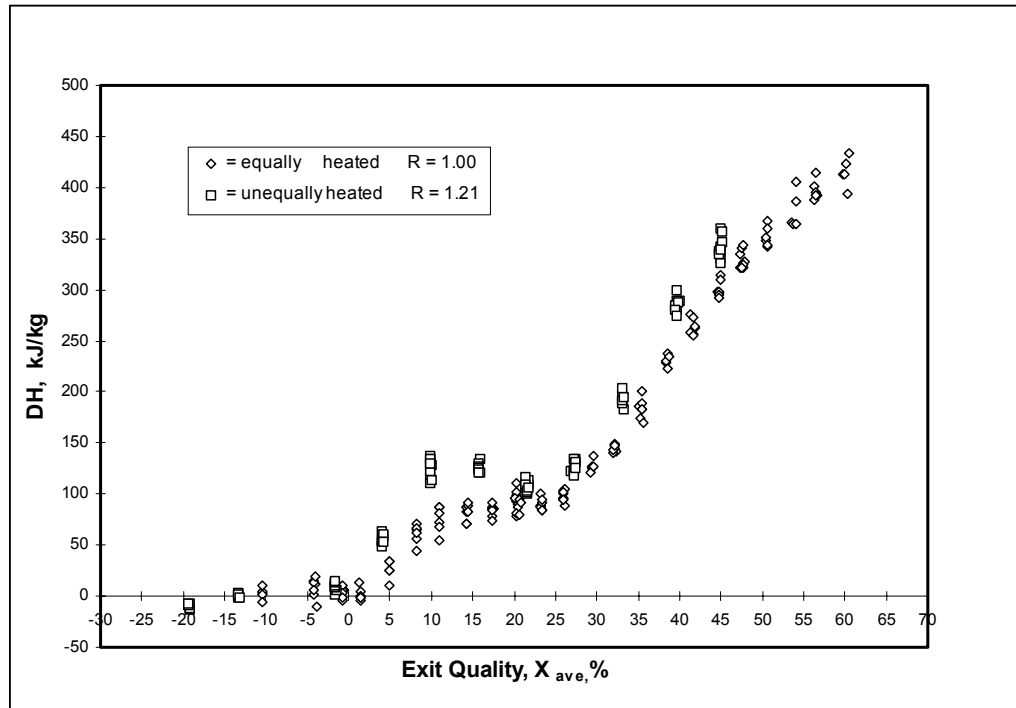


Figure 7: Enthalpy/Void Migration vs. Exit Quality at $P = 10.0$ MPa and $G = 1.6$ Mg/m²s

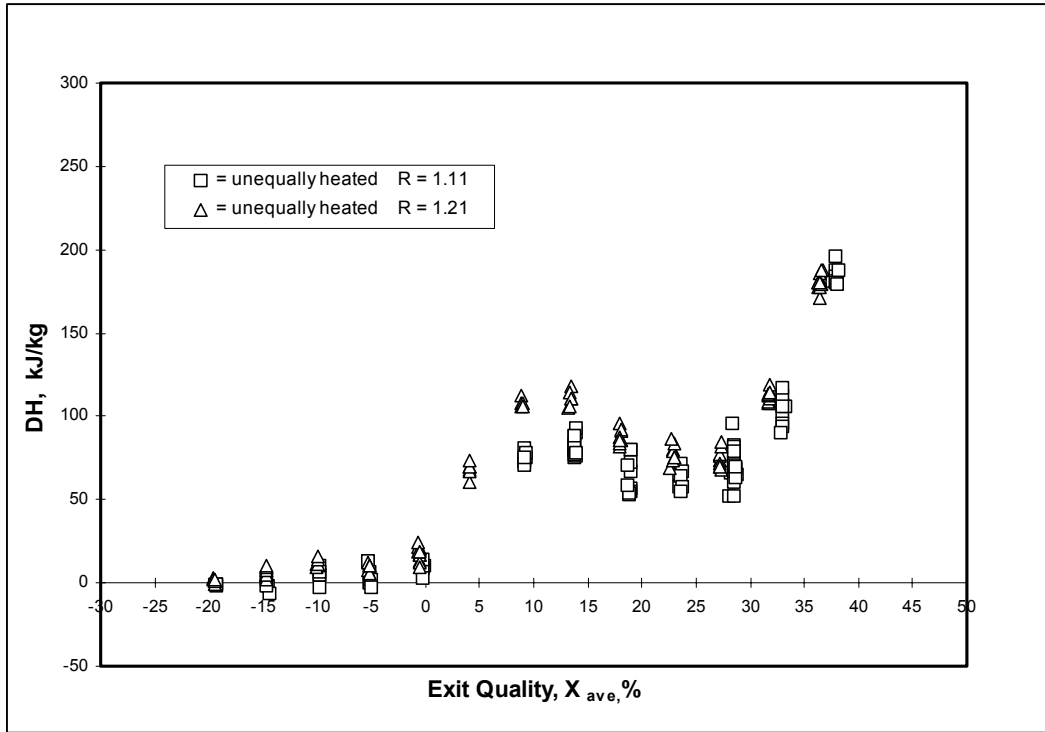


Figure 8: Enthalpy/Void Migration vs. Exit Quality at $P = 10.0$ MPa and $G = 2.0$ Mg/m²s

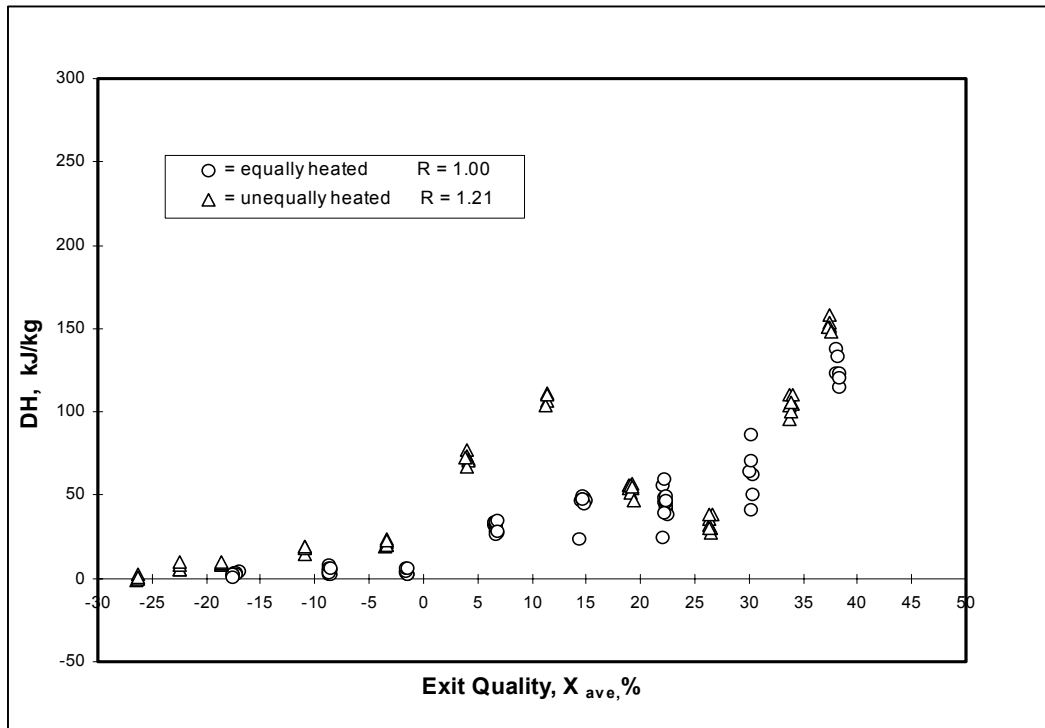


Figure 9: Enthalpy/Void Migration vs. Exit Quality at $P = 10.0$ MPa and $G = 2.5$ Mg/m²s

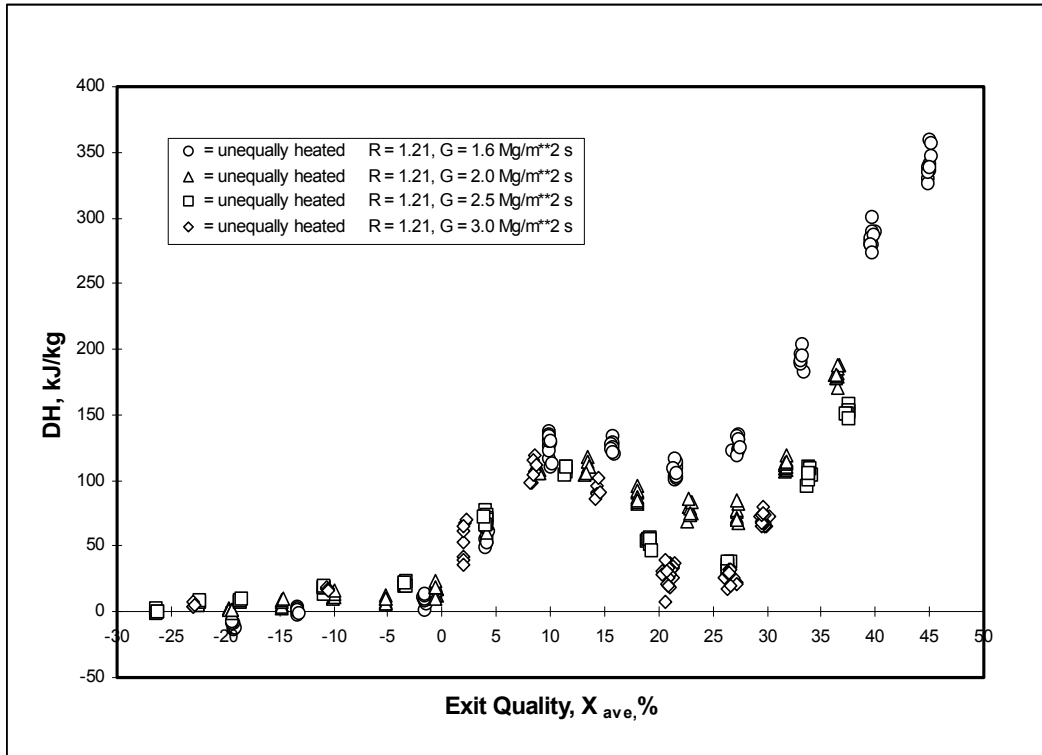


Figure 10: Enthalpy/Void Migration vs. Exit Quality at P = 10.0 MPa

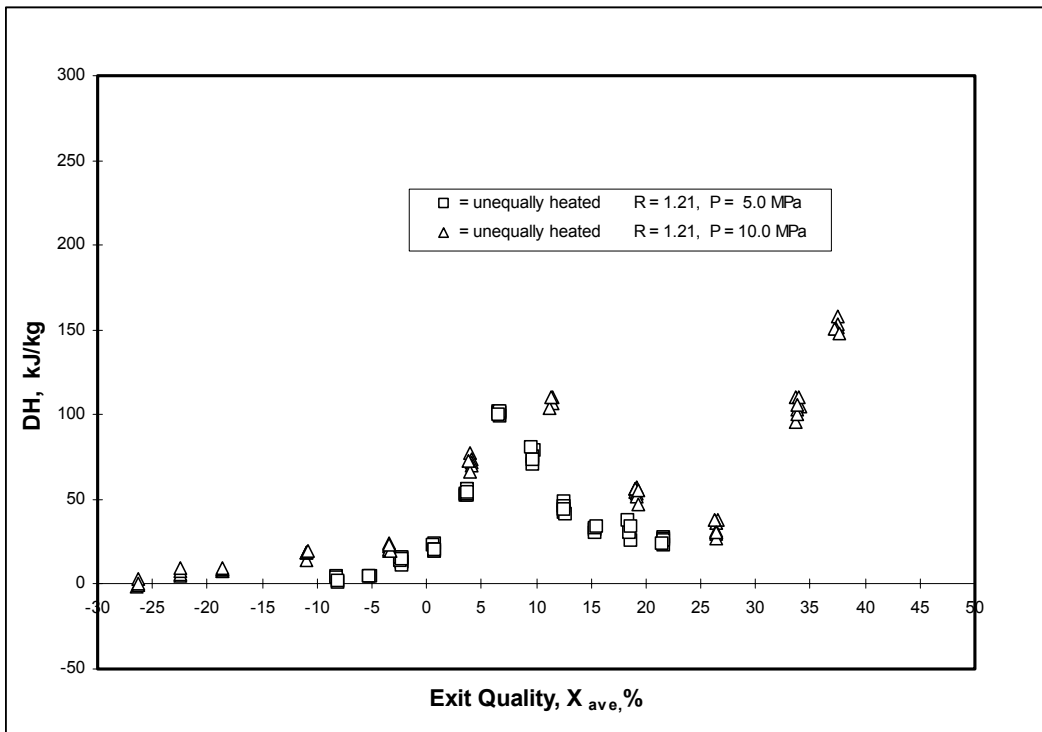


Figure 11: Enthalpy/Void Migration vs. Exit Quality at P = 5.0 and 10.0 MPa, G = 2.5 Mg/m²s